

Molecular basis of influenza hemagglutinin inhibition with an entry-blocker peptide by computational docking and mass spectrometry

Robert Lu, Patrick Müller and Kevin M Downard

Antiviral Chemistry and Chemotherapy
2015, Vol. 24(3–4) 109–117

© The Author(s) 2016

Reprints and permissions:

sagepub.co.uk/journalsPermissions.nav

DOI: 10.1177/2040206615622920

avc.sagepub.com



Abstract

Background: The increased resistance of circulating strains to current antiviral inhibitors of the influenza virus necessitates that new antivirals and their mode of action are identified. Influenza hemagglutinin is an ideal target given inhibitors of its function can block the entry of the virus into host cells during the early stages of replication. This article describes the molecular basis for the inhibition of H1 and H5 hemagglutinin by an entry-blocker peptide using companion molecular docking and mass spectrometry-based experiments.

Methods: A combination of hemagglutination inhibition assays, computational molecular docking and a novel mass spectrometry-based approach are employed to explore the mode of action of the entry-blocker peptide at a molecular level.

Results: The entry-blocker peptide is shown to be able to maximally inhibit blood cell hemagglutination at a concentration of between 6.4 and 9.2 μM . The molecular basis for this inhibition is derived from the binding of the peptide to hemagglutinin in the vicinity of the reported sialic acid binding site surrounded by an α -helix (190-helix) and two loop (130-loop and 220-loop) regions in the case of a H1 hemagglutinin and the second loop region in the case of a H5 hemagglutinin.

Conclusions: The results support the recognized potential of the entry-blocker peptide as an effective antiviral agent that can inhibit the early stages of viral replication and further illustrate the power of a combination of docking and a mass spectrometry approach to screen the molecular basis of new antiviral inhibitors to the influenza virus.

Keywords

Hemagglutinin, inhibition, peptide, influenza, molecular docking, mass spectrometry

Date received: 14 October 2015; accepted: 24 November 2015

Introduction

Hemagglutinin (HA) is a glycoprotein located on the surface of influenza virus particles.¹ The encoded precursor protein, HA0, is synthesized as a single protein and cleaved by a cellular protease into the HA1 and HA2 subunits. The HA1 subunit contains the sialic acid receptor-binding pocket and antigenic epitopes, while the first 23 N-terminal residues of the HA2 subunit comprise the fusion peptide (FP). The HA1 and HA2 subunits are linked together by means of a disulphide bond. Three of these bridged HA molecules associate to form a homotrimer on the surface of a virus particle that represents the functional HA.²

Influenza virus infection of host cells begins with the binding of HA to sialic acid receptors on the surface of host cells. Once bound, the protein facilitates entry of

the viral RNA into the host cells by causing the fusion of the endosomal membrane. To release virus genomes into the cytoplasm, fusion between the viral envelope and endosome membrane occurs in an acidic environment. This triggers an irreversibly conformational change in HA. Under these acidic pH conditions, the hydrophobic FP at the N-terminus of HA2 is released from its buried position.³ It interacts with the endosomal membrane and initiates a series of conformational

University of New South Wales, Sydney, Australia

Corresponding author:

Kevin M Downard, Prince of Wales Clinical School, University of New South Wales, Sydney, NSW 2052, Australia.

Email: kevin.downard@unsw.edu.au

rearrangements of HA2 that leads to membrane fusion and release of viral RNA into the host cells.

The blocking of HA-mediated fusion is one strategy used for the design of antiviral inhibitors against the virus that target influenza HA.⁴ Another involves blocking the entry of the virus into host cells by targeting the surface of the influenza HA.⁵ There are benefits in preventing viral replication early in the infection cycle,^{6,7} particularly in light of an increasing number of circulating strains of influenza that are resistant to the current neuraminidase inhibitors oseltamivir and zanamivir.⁸ A range of inhibitors to influenza HA,⁹ including peptide-based inhibitors,¹⁰ have been reported and some, such as arbidol,¹¹ have been approved for administration in humans.

A previous study has identified an entry-blocker (EB) peptide, derived from a fibroblast growth factor signal sequence, which displayed broad anti-influenza virus activity both *in vitro* and *in vivo*.¹² The full length, 20 amino acid residue peptide inhibits influenza virus infection by preventing virus attachment to host cells, though the molecular basis for its mode of action is unknown. A subsequent study, by the same authors,¹³ reported on the minimal, truncated EB sequence required to retain the antiviral activity and inhibitory concentration (IC₅₀) of the full length peptide so as to simplify its synthesis and reduce potential production costs.

This study examines the molecular basis of the inhibitory properties of EB peptide against both H1 and H5 HA. Parallel computational molecular docking and mass spectrometry-based experiments, in conjunction with inhibition assays, have been employed in approaches akin to those of a recent report from this laboratory that investigated the molecular basis¹⁴ of another HA inhibitor, arbidol.¹¹ The mass spectrometry approach¹⁵ has been successfully applied to study the binding of a range of antiviral inhibitors to influenza neuraminidase,^{16–19} thus providing a solid foundation for this study.

Materials and methods

Recombinant HA, vaccines and EB peptide

Recombinant H1 and H5 HA based on the sequences derived for the A/California/04/2009 (H1N1) and A/Vietnam/1194/2004 (H5N1) strains were purchased from Sino Biologicals (Beijing, China). Lyophilised protein was reconstituted in 200–400 µL of purified water to achieve a stock concentration of 0.25 µg/mL.

The PanVax split virion vaccine formulated against the H1N1 2009 pandemic strains was provided by CSL Biotherapies, CSL Limited (Parkville, Victoria, Australia), while the H5N1 whole virion vaccine

(A/Vietnam/1203/2004) was obtained from BEI Resources (Manassas, VA, USA).

The EB peptide (of sequence RKKAAVALLP-AVLLALLAP and average molecular mass 2084.65) was synthesized and purchased from Auspep (Melbourne, Australia).

Hemagglutination inhibition assays

Hemagglutination inhibition (HI) assays were performed in 96-well V-bottom microtitre plates using heparinised chicken red blood cells (RBCs) obtained from Westmead Hospital, Sydney. Starting vaccine concentrations equivalent to 2.67 µg/mL of HA were serially diluted to ascertain the amount of virus required to achieve four times the minimal agglutination concentration or hemagglutination units (HAU). EB peptide was dissolved in PBS with a starting concentration of between 13 and 20 µg/mL. Inhibitor titrations were performed in the presence and absence of four HAU of vaccine, to ensure agglutination was virus dependent, by serially diluting the inhibitor from the highest dose concentration, representing a concentration 10-fold higher than the reported IC₅₀ value (*in-vitro*), to the concentration at which agglutination inhibition was complete or near complete. Dilutions of inhibitor were pre-incubated with four HAU of vaccine for 15 min followed by the addition of a RBC solution (0.67% w/v, total volume 150 µL) for 1 h at 37°C.

Computational molecular docking of truncated EB peptide (EB^{B12-NBR}) to H1 and H5 HA

Molecular docking experiments were performed using the AutoDock v4.2.6 program on a Dell Optiplex personal computer fitted with an Intel i5, 2.5 GHz core processor running the Windows 7 operating system. The X-ray structures for H1 and H5 HA (3LZG and 3ZNM, respectively) were obtained from the protein data bank (PDB). Due to computational constraints, the protein was docked with the truncated version of the EB peptide, EB^{B12-NBR} (of sequence ALLVALLAP) representing the minimal active peptide, without the terminal RKK residues to aid solubility and any internal deletions.¹³

A 3D structure for the full length EB peptide was constructed using the MarvinSketch chemical editor (Chemaxon, Budapest, Hungary) from its input sequence. The structure was optimized using the 3D geometry and optimization utilities, using default parameters, and exported as a PDB file. This file was edited to remove the terminal residues. The remaining truncated peptide displayed a partial helical structure.

The truncated EB peptide and HA protein structures were docked in two stages using AutoDock. First, blind rigid molecule dockings were performed across the

HA1 head region a cubic grid of 126 points per side in size at a resolution of 0.375 Å. In the second refined docking experiment, grids centred on putative binding sites determined from the first docking were used with a grid size of 70 points per side at the same resolution. The following docking parameters were employed: *ga_num_evals* 25 million, *pop_size* 300, quaternion step size 50° and torsion step size 50°. In all dockings, 200 conformations were generated per run with a total of three replicate runs performed for each putative docking site.

The three lowest binding free energy conformers were filtered by clustering using a *rmstol* (RMSD tolerance) of 10.0 Å. The models were analysed further with the Pymol molecular viewer (DeLano Scientific, San Francisco, USA).

Incubation of EB peptide with H1 and H5 HA followed by proteolytic digestion

Deglycosylation of recombinant HA with 1.2 units of recombinant peptide-N-glycosidase F (PNGaseF) (Roche Diagnostics, Sydney, Australia) was verified by SDS-PAGE. A solution of deglycosylated protein, equivalent to 5 µg HA, in 25 mM ammonium bicarbonate was left untreated or treated with a 10 molar excess of EB peptide inhibitor for each subtype (H1 and H5) and incubated for 2 h at 37°C.

Limited proteolysis of untreated and full length EB peptide-treated HA was performed by the stepwise addition of ~1:30 mole ratio (60 ng enzyme per µg HA) of sequencing-grade endoproteinase Glu-C from *Staphylococcus aureus* V8 (Sigma-Aldrich, Sydney, Australia) and modified porcine trypsin endoproteinase (Promega Corporation, Sydney, Australia). Digests were carried out sequentially to minimise enzyme autolysis and cross-digestion products. Overnight Glu-C digestion in 25 mM ammonium bicarbonate buffered solution was performed first as it is particularly sensitive to proteolysis (against itself and other endoproteinases). The following day, samples were incubated overnight with trypsin also in 25 mM ammonium bicarbonate solution. The released peptides were reduced and alkylated in a solution containing 5 mM dithiothreitol and 10 mM iodoacetamide and desalted using C18 ZipTip™ (EMD Millipore, Billerica, MA, USA) 10 µL tips. The extracted peptides were completely dried in a Labconco Centrivap (Labconco, Kansas City, MO, USA) prior to matrix-assisted laser desorption/ionization (MALDI-MS) analysis.

High-resolution MALDI-MS of HA peptides

Reconstituted peptides (~1.6 µg/µL in 3 µL water) were diluted in a 5 mg/mL solution of α -cyano-4-hydroxycinnamic acid (8 µL containing 50% by volume

acetonitrile and 0.1% trifluoroacetic acid); 1 µL of combined sample and matrix solution was spotted twice onto a Bruker MTP Anchorchip 400/384 TF plate (Bruker Daltonics, Billerica, MA, USA).

High-resolution FT-ICR mass spectra were obtained on a 7T Bruker APEX-Qe instrument (Bruker Daltonics, Billerica, MA, USA) in the positive ion-mode as previously described.²⁰ Spectra were acquired from an average of six scans using a broadband excitation and plotted herein in the *m/z* range of 500–3000.

Analysis of MALDI-MS data to identify binding segments

Peak lists derived from the acquired mass spectra were deisotoped, and the monoisotopic masses associated with HA-derived peptides were identified by matching the peak masses, using an error tolerance of 10 ppm, to those theoretically generated using the MS-FIT algorithm (UCSF Protein Prospector webserver). Sequence coverages of 40.9% (17 matched peptides) and 29% (12 matched) were obtained for H1 and H5 HA, respectively. The average relative peak intensities of the matched HA peptides, across replicate data for untreated and treated HA samples, were compared. Those whose relative intensities decreased by greater than 10% (absolute) were deemed to be bound to EB peptide based on established errors from past experiments.^{15–19} The PRISM algorithm²¹ was employed to assist with this analysis. Minor products associated with the partial digestion of EB peptide are denoted (*) in the EB-treated mass spectra.

Results

HA inhibition assays

Viruses adhere to or agglutinate RBCs by means of the HA glycoprotein. Compounds that bind to HA can inhibit this agglutination. This leads to the pooling or buttoning of blood cells in the base of the wells of a titre plate.

HIA assays were performed with increasing concentrations of EB peptide up to 26.5 or 20 µg/mL. Inhibition of agglutination was apparent from an increase in density of RBCs in the bottom of the well with increasing concentrations of EB peptide (Figure 1) using four HAU equivalents of H1N1 virus. Although incomplete even at high concentrations, a concentration of 13.3 µg/mL or 6.4 µM was established as the endpoint of the effect. At and above this concentration, some peptide-induced hemagglutination was observed based on results for RBCs treated only with the peptide, which masks complete inhibition in the presence of virus. Drug-induced, dose-dependent hemagglutination

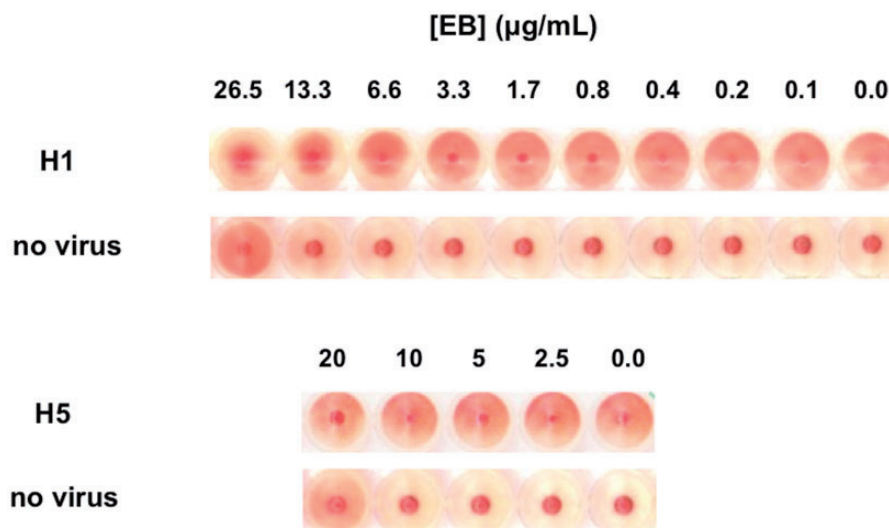


Figure 1. Hemagglutinin inhibition assays (HIA) using serial dilutions of full length EB peptide against standardized solutions (containing four HAU equivalents) of H1N1 (Panvax containing a A/California/07/09-like strain) and H5N1 (containing a A/Vietnam/1203/2004 strain) vaccines.

EB: entry-blocker.

has previously been reported for both peptides and pharmaceutical compounds.^{22,23}

In the case of the H5N1 virus (Figure 1), partial agglutination was apparent at between 2.5 µg/mL with near complete inhibition detected at approximately 20 µg/mL or 9.2 µM. At and above this concentration, peptide-induced hemagglutination was observed for RBCs treated only with the peptide and no virus.

Computational molecular docking

The ability of EB peptide to inhibit hemagglutination suggested that it binds to the accessible HA1 domain atop the HA protein. Molecular docking to H1 and H5 HA was performed in two stages. The first involved blind docking across large overlapping sections of the entire HA1 head region of the PDB structures for H1 and H5 HA (3LZG and 3ZNM). This established putative binding sites at which more refined docking was performed to obtain the lowest free energy model.

Due to the computational complexity associated with docking large ligands to proteins, the truncated version designated EB^{B12-NBR} (of sequence AVLLALLAP) was used. This compromise is reasonable given that it has been reported that the N-terminal residues are only considered necessary for peptide solubility,¹³ not binding, and thus can be ignored during *in-silico*-based docking procedures. The truncated peptide EB^{B12-NBR} has been previously established in structure-activity relation studies as being the minimal segment that retained near complete activity *in-vitro*.¹³

The lowest energy (−8.66 kcal/mol) conformer of EB^{B12-NBR} bound to H1 HA has the peptide located

within a cavity of the HA1 head region where it interacts with neighbouring HA1 subunits within the trimer (Figure 2(a)). In this top-ranked conformer, the peptide is in closest contact with HA residues 96-99, 208-213, and Tyr-230. Note that the residues are numbered according to the sequence for the recombinant H1 protein and may differ from those within the PDB structure file. Much the same is true of the second-ranked conformer, though here, the peptide is less elongated and orientated at approximately 180° about both its vertical and horizontal axis from the top-ranked orientation (Figure 2(b)).

The third-ranked conformer was with only a marginally higher binding energy (−6.76 kcal/mol), but has the peptide located inside a pocket surrounded by residues of a single HA1 unit. In this case, the peptide is in the vicinity of HA residues 130–132, 146, 183–186 and 222–227. This model has the EB peptide located within the reported sialic acid binding site surrounded by an α -helix (190-helix) and two loop (130-loop and 220-loop) regions (Figure 3). This binding site contains residues that are conserved across both H1 and H5 serotypes.²⁴

Docking of the EB peptide to H5 HA yields two top-ranked conformers in which the peptide also resides in this region of the protein. Both have similar binding free energies of −6.04 and −5.28 kcal/mol. The first exhibits the peptide in a more elongated orientation with its C-terminal residues in closest contact with residues 86-95, and Ser133 and Asn220 of two loop regions within a single HA1 subunit. In the second-ranked conformer, the peptide is more twisted and is in close proximity to H5 residues 71-73, 205-212 and 229-230.

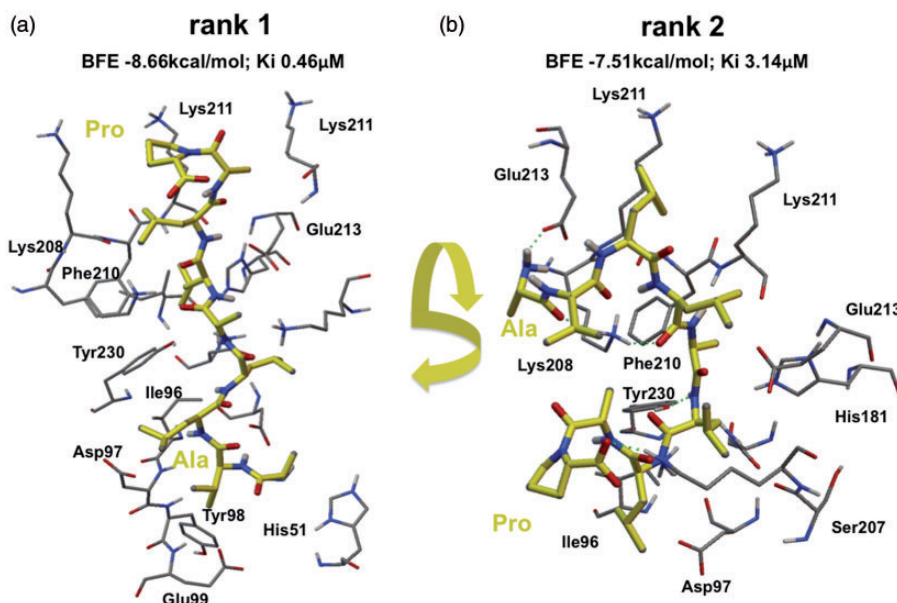


Figure 2. Top-ranked (ranks 1 and 2) conformers of EB^{B12-NBR} bound to H1 hemagglutinin. Note that the numbering is based on recombinant hemagglutinin sequence.

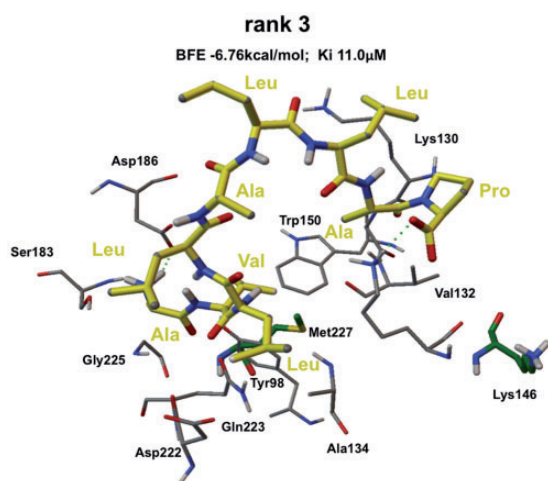


Figure 3. Third-ranked (rank 3) conformer of EB^{B12-NBR} bound to H1 hemagglutinin. Note that the numbering is based on recombinant hemagglutinin sequence.

Interaction of H1 and H5 HA with full length EB peptide by MALDI-MS

The interaction of full length EB peptide with H1 and H5 HA was investigated experimentally in parallel by mass spectrometry. The MS-based approach has been previously employed in this laboratory to study the binding of antiviral inhibitors to their target proteins^{14,16–19} and is based on a molecular-based method originally deployed to study the antigenicity of virus strains.¹⁵

In brief, recombinant H1 and H5 HA were each digested sequentially with endoproteinase GluC and trypsin before and after their incubation with full length EB peptide. Cleavage residues in close proximity or bound to the peptide will be partially or fully shielded from the proteases resulting in a reduction in their relative levels or absence in the spectra of the EB peptide-treated HA samples compared those for the untreated control samples.

Representative mass spectra of untreated and EB peptide-treated H1 HA after proteolysis are shown in Figure 5. The most apparent differences in peak intensity in these spectra appear in the HA peptide ions at m/z 885, 1615, 1785 and 2105. Table 1 lists the average peak intensities and standard deviations across spectra from replicate experiments. Beyond the established error for these experiments (of $\pm 10\%$),^{14–19} only four peptides have relative peak intensities which decrease by greater than 10% (absolute). Of these, two peptides at m/z 1615 and 2105 contain residues from the same segment of the protein (227–239/243), the latter associated with an additional miscleaved site. These results favour the third ranked conformer (Figure 3) where residues 222–227 containing the N-terminal cleavage site (226–227) are in close proximity to the N-terminal residues AVL of the truncated EB^{B12-NBR} peptide. This results in a reduction in the relative intensity of the peptides comprising residues 227–239 and 227–243 of 11.81% and 13.80% (absolute), respectively.

In this conformer, lysine at position 146 is also proximal to the peptide (Figure 3) that shields the cleavage

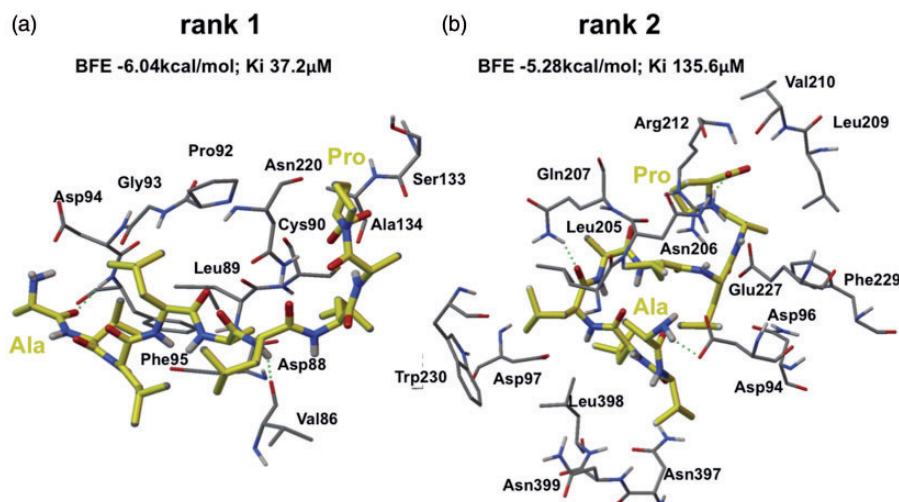


Figure 4. Top-ranked (ranks 1 and 2) conformers of EB^{B12-NBR} bound to H5 hemagglutinin. Note that the numbering is based on recombinant hemagglutinin sequence.

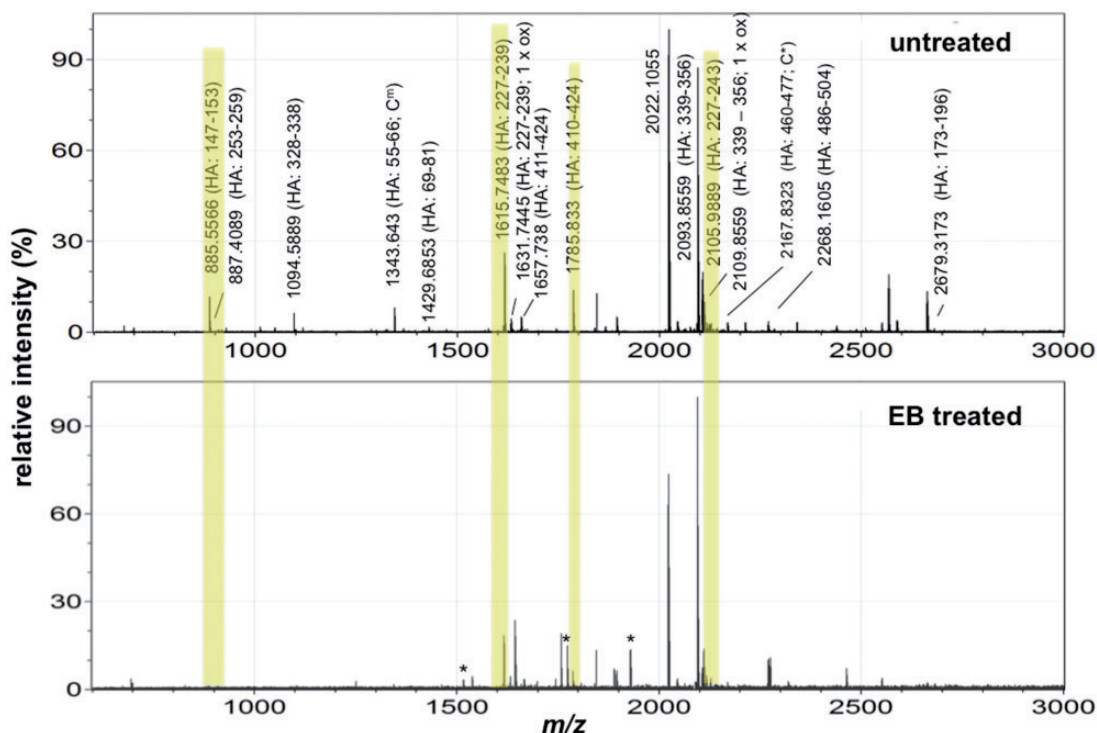


Figure 5. Representative MALDI mass spectra of GluC/trypsin peptides released from untreated and full length EB peptide-treated H1 hemagglutinin. C^m: a carbamidomethylated peptide; ox : oxidised form.

site at HA residues 146 and 147 from proteolysis with trypsin resulting in a reduction (13.14% absolute) in the relative intensity of the released peptide comprising residues 147–153.

Representative mass spectra for untreated and EB peptide-treated H5 HA after proteolysis are shown in Figure 6. In this case, only a single peak associated with

a segment of H5 HA undergoes a reduction in its relative peak intensity exceeding 10% (absolute). Based on the results of replicate data (Table 2), this peptide corresponding to HA residues 228–242 decreases in relative peak intensity by 54.29%.

These results favour the second-ranked conformer (Figure 4, rank 2) where the glutamic acid residue at

Table 1. MALDI-MS peak intensity data for the GluC/tryptic peptides released from untreated and EB peptide-treated H1 hemagglutinin.

<i>m/z</i>	Residues ^a	Sequence ^b	Untreated HI average peak intensity ^c	Peptide-treated HI average peak intensity ^c	Difference in average peak intensity
885.5566	147–153	(K)NLIWLVK(K)	14.56 (8.45)	1.42 (1.88)	13.14
887.4089	253–259	(R)YAFAMER(N)	4.62 (2.00)	0.13 (0.30)	4.49
1094.5889	328–338	(R)GLFGAIAGFIE(G)	7.83 (3.71)	0.72 (0.86)	7.11
1343.6430	55–66	(K)CmNIAGWILGNPE(C)	10.18 (3.72)	1.76 (0.18)	8.42
1429.6853	69–81	(E)SLSTASSWSYIVE(T)	2.33 (0.76)	0.88 (1.00)	1.45
1615.7483	227–239	(R)MNYWTLVEPGDK(I)	30.21 (5.31)	18.40 (2.24)	11.81
1631.7445	227–239 ^d	(R)MNYWTLVEPGDK(I)	3.21 (1.09)	2.33 (1.67)	0.88
1632.7168	55–68	(K)CNIAGWILGNPECE(S)	5.54 (2.29)	1.03 (0.80)	4.51
1657.7382	411–424	(K)VDDGFLDIWTYNAE(L)	6.01 (1.05)	0.64 (0.18)	5.37
1785.8344	410–424	(K)KVDDGFLDIWTYNAE(L)	16.15 (3.25)	4.03 (0.57)	12.12
1894.0086	396–410	(K)EFNHLEKRIENLNKK(V)	5.60 (1.47)	5.08 (0.46)	0.52
2062.9848	188–205	(D)QQSLYQNADTYVFGSSR(Y)	1.60 (0.38)	1.22 (1.44)	0.42
2093.8578	339–356	(E)GGWTGMVDGWYGYHHQNE(Q)	100.00 (0.00)	100.00 (0.00)	0.00
2105.9929	227–243	(R)MNYWTLVEPGDKITFE(A)	21.34 (4.14)	7.54 (1.65)	13.80
2109.8559	339–356 ^d	(E)GGWTGMVDGWYGYHHQNE(Q)	9.14 (1.63)	13.97 (2.78)	−4.83
2121.987	227–243	(R)MNYWTLVEPGDKITFE(A)	3.03 (0.68)	0.88 (0.42)	2.15
2167.8323	460–477	(E)IGNGCFEFYHKCDNTCME(S)	3.92 (1.44)	2.52 (0.54)	1.40
2268.1605	486–504	(D)YPKYSEEAKLNREEIDGVK(L)	4.37 (0.77)	9.95 (1.89)	−5.58
2679.3173	173–196	(E)VLVLWGIHPSTSADQQSLYQNAD(T)	1.45 (0.41)	1.71 (0.23)	−0.26

^aNumbering is based on the HA0 hemagglutinin sequence.

^bResidues aside the cleavage site are shown in brackets where C^m indicates a carbamidomethylated cysteine residue.

^cValues represent an average of duplicate data with standard deviations shown in brackets.

^dA monooxidized (likely at the methionine residue) form of the peptide

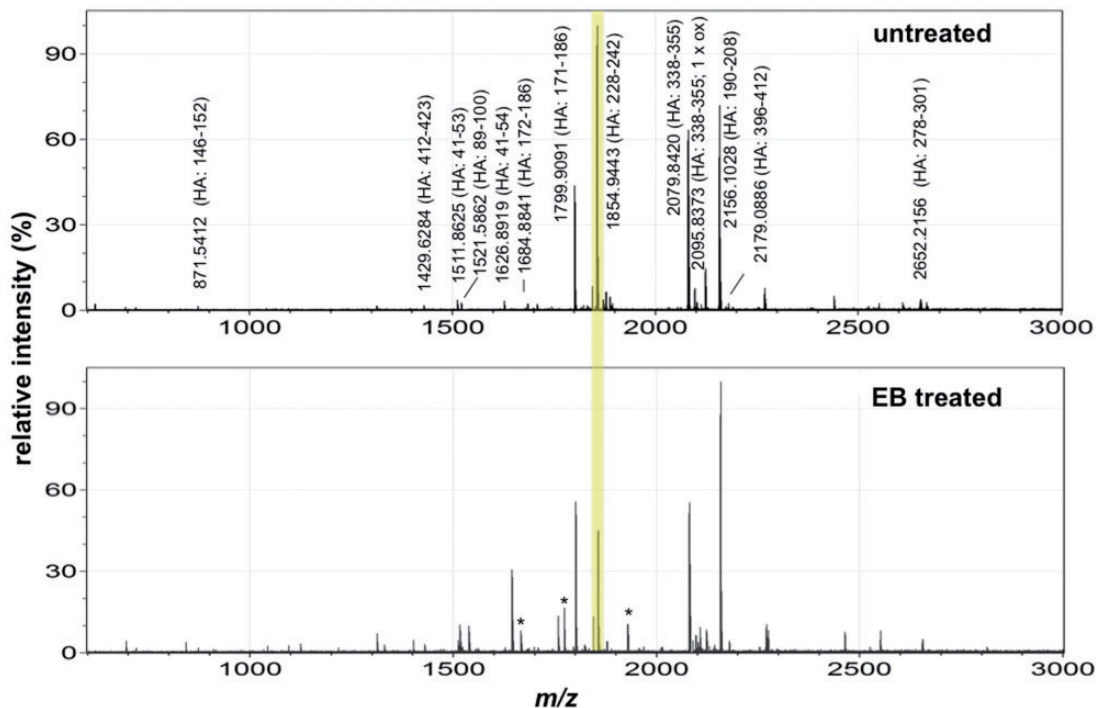


Figure 6. Representative MALDI mass spectra of GluC/tryptic peptides released from untreated and full length EB peptide-treated H5 hemagglutinin.
ox : an oxidised peptide.

Table 2. MALDI-MS peak intensity data for the GluC/tryptic peptides released from untreated and EB peptide-treated H5 hemagglutinin.

<i>m/z</i>	Residues ^a	Sequence ^b	Untreated H5 average peak intensity ^c	EB peptide-treated H5 average peak intensity ^c	Difference in average peak intensity
871.5412	146–152	(R)NVVWLIK(K)	1.55 (0.86)	2.04 (0.57)	–0.49
1429.6284	412–423	(E)DGFLDVWTYNAE(L)	1.95 (0.49)	3.26 (0.38)	–1.31
1511.8625	41–53	(K)LCDLDGVKPLILR(D)	3.62 (0.47)	4.45 (1.45)	–0.83
1521.5862	89–100	(D)LCYPGDFNDYEE(L)	2.86 (0.36)	2.34 (0.15)	0.52
1626.8919	41–54	(K)LCDLDGVKPLILRD(C)	3.40 (0.06)	2.18 (0.10)	1.22
1684.8841	172–186	(D)LLVLWGIHHPNDAAE(Q)	2.42 (0.43)	2.77 (0.71)	–0.35
1799.9091	171–186	(E)DLLVLWGIHHPNDAAE(Q)	43.88 (2.73)	54.44 (6.98)	–10.56
1854.9443	228–242	(E)FFWTILKPNDAINFE(S)	100.00 (0.00)	45.71 (1.14)	54.29
2079.8420	338–355	(E)GGWQGMVDGWYGYHHSNE(Q)	63.45 (3.98)	59.72 (20.35)	3.73
2095.8373	338–355 ^d	(E)GGWQGMVDGWYGYHHSNE(Q)	8.13 (1.48)	6.90 (0.48)	1.23
2156.1028	190–208	(K)LYQNPTTYSVGTSTLNQR(L)	72.74 (8.19)	100.00 (0.00)	–27.26
2179.0886	396–412	(E)FNNLERRIENLNKKMED(G)	2.56 (0.08)	4.28 (0.59)	–1.72
2652.2156	278–301	(K)CQTPMGAINSSMPFHNIHPLTIGE(C)	3.83 (0.92)	5.77 (1.70)	–1.94

^aNumbering is based on the HA0 hemagglutinin sequence.

^bResidues aside the cleavage site are shown in brackets.

^cValues represent an average of duplicate data with standard deviations shown in brackets.

^dA monooxidized (likely at the methionine residue) form of the peptide.

position 228 is in close proximity to the most C-terminal alanine residue of the truncated EB^{B12-NBR} peptide. This reduces the accessibility of endoprotease GluC to the cleavage site between residues 227 and 228.

No such restriction is observed at the GluC between residues 395 and 396. The phenylalanine residue at position 396 is located directly below the asparagine residue at position 397 in second-ranked conformer (Figure 4, rank 2), away from the location of the EB peptide. Consequently, the latter has no impact on the cleavage of this site by the endoproteinase and the relative levels of the HA peptide comprising residues 396–412 (Table 2).

Discussion

The molecular basis of an EB peptide, previously reported to inhibit the attachment of the influenza virus to host cells, has been explored, theoretically and experimentally, by a combination of computational molecular docking and mass spectrometry. The results of these disparate approaches are largely in accord, and demonstrate that the peptide binds to H1 and H5 HA in the vicinity of the reported sialic acid receptor binding site, particularly impacting on the accessibility of residues in the 220-loop region.

The combined results support the recognized potential of the EB peptide as an effective antiviral agent that can inhibit the early stages of viral replication. This study, together with other published work from this

laboratory,^{14,16–19} further demonstrates the power of a combination of docking and a MALDI-MS approach, with high-throughput capability, to explore the potential of new antiviral inhibitors through analysis of their interaction with viral protein targets.

Acknowledgements

The authors are grateful to Dr. Nick Proschogo who performed some of the MALDI-MS analyses and Dr. Janette Taylor and Prof. Dominic Dwyer, Westmead Hospital, Sydney who provided the red blood cells used in this study.

Declaration of conflicting interests

The author(s) declared no potential conflicts of interest with respect to the research, authorship, and/or publication of this article.

Funding

The author(s) disclosed receipt of the following financial support for the research, authorship, and/or publication of this article: Financial support for this research was provided by the Australian Research Council in the form of a Discovery Project grant (DP140100591) awarded to K. Downard.

References

- Gamblin SJ and Skehel JJ. Influenza hemagglutinin and neuraminidase membrane glycoproteins. *J Biol Chem* 2010; 285: 28403–28409.

2. Sriwilajaroen N and Suzuki Y. Molecular basis of the structure and function of H1 hemagglutinin of influenza virus. *Proc Jpn Acad Ser B Phys Biol Sci* 2012; 88: 226–249.
3. Schoch C and Blumenthal R. Role of the fusion peptide sequence in initial stages of influenza hemagglutinin-induced cell fusion. *J Biol Chem* 1993; 268: 9267–9274.
4. Shen X, Zhang X and Liu S. Novel hemagglutinin-based influenza virus inhibitors. *J Thorac Dis* 2013; 5: S149–S159.
5. Yang J, Li M, Shen X, et al. Influenza A virus entry inhibitors targeting the hemagglutinin. *Viruses* 2013; 5: 352–373.
6. Kalyan D, Aramini JM, Ma L-C, et al. Structures of influenza A proteins and insights into antiviral drug targets. *Nat Struct Mol Biol* 2010; 17: 530–538.
7. Das K. Antivirals targeting influenza A virus. *J Med Chem* 2012; 55: 6263–6277.
8. van der Vries E, Schutten M, Fraaij P, et al. Influenza virus resistance to antiviral therapy. *Adv Pharmacol* 2013; 67: 217–246.
9. Vanderlinden E and Naesens L. Emerging antiviral strategies to interfere with influenza virus entry. *Med Res Rev* 2014; 34: 301–339.
10. Matsubara T, Onishi A, Saito T, et al. Sialic acid-mimic peptides as hemagglutinin inhibitors for anti-influenza therapy. *J Med Chem* 2010; 53: 4441–4449.
11. Blaising J, Polyak SJ and Pécheur EI. Arbidol as a broad-spectrum antiviral: an update. *Antiviral Res* 2014; 107: 84–94.
12. Jones JC, Turpin EA, Bultmann H, et al. Inhibition of influenza virus infection by a novel antiviral peptide that targets viral attachment to cells. *J Virol* 2006; 80: 11960–11967.
13. Jones JC, Settles EW, Brandt CR, et al. Identification of the minimal active sequence of an anti-influenza virus peptide. *Antimicrob Agents Chemother* 2011; 55: 1810–1813.
14. Nasser Z, Swaminathan K, Müller P, et al. *In-vitro* inhibition of the influenza virus with the anti-viral inhibitor arbidol by a proteomics based approach with mass spectrometry. *Antiviral Res* 2013; 100: 399–406.
15. Kiselar JG and Downard KM. Antigenic surveillance of the influenza virus by mass spectrometry. *Biochemistry* 1999; 43: 14185–14191.
16. Swaminathan K and Downard KM. Anti-viral inhibitor binding to influenza neuraminidase by MALDI mass spectrometry. *Anal Chem* 2012; 84: 3725–3730.
17. Swaminathan K, Dyason JC, Maggioni A, et al. Binding of a natural anthocyanin inhibitor to influenza neuraminidase by mass spectrometry. *Anal Bioanal Chem* 2013; 405: 6563–6572.
18. Swaminathan K, Müller P and Downard KM. Substituent effects on the binding of natural product anthocyanidin inhibitors to influenza neuraminidase with mass spectrometry. *Anal Chim Acta* 2014; 828: 61–69.
19. Müller P and Downard KM. Catechins inhibit influenza neuraminidase and its molecular basis with mass spectrometry. *J Pharm Biomed Anal* 2015; 111: 222–230.
20. Schwahn AB, Wong JWH and Downard KM. Subtyping of the influenza virus by high resolution mass spectrometry. *Anal Chem* 2009; 81: 3500–3506.
21. Ho JW, Morrissey B and Downard KM. A computer algorithm for the identification of protein interactions from the spectra of masses (PRISM). *J Am Soc Mass Spectrom* 2007; 18: 563–566.
22. Moreau E, Domuradob M, Chaponb P, et al. Biocompatibility of polycations: in vitro agglutination and lysis of red blood cells and in vivo toxicity. *J Drug Target* 2002; 10: 161–173.
23. de Lima JM, Sarmiento RR, de Souza JR, et al. Evaluation of hemagglutination activity of chitosan nanoparticles using human erythrocytes. *Biomed Res Int* 2015; 2015: 247965.
24. Stevens J, Blixt O, Tumpey TM, et al. Structure and receptor specificity of the hemagglutinin from an H5N1 influenza virus. *Science* 2006; 312: 404–410.